Supplemental Information

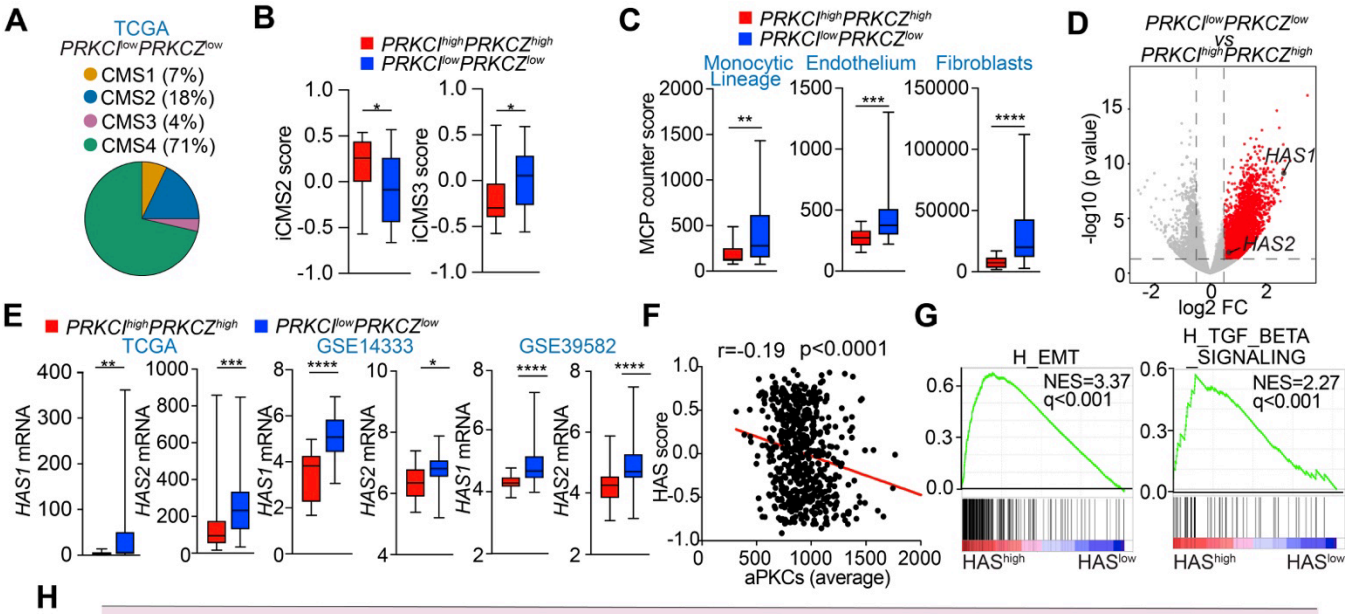

H

Variables	All patients (n=343)	aPKCs-high HA-positive (n=122)	aPKCs-high HA-negative (n=47)	aPKCs-low HA-positive (n=150)	aPKCs-low HA-negative (n=24)	p value
Age, years		66.9 (11.9)	69.9 (10.8)	66.4 (10.6)	67.1 (9.7)	0.302 ns
Age≥65	210	75 (35.7)	33 (15.7)	88 (41.9)	14 (6.7)	0.555 ns
Sex						
Male	176	53 (30.0)	28 (15.9)	83 (47.2)	12 (6.8)	0.152 ns
Clinical stage						
II	171	54 (31.6)	30 (17.5)	74 (43.3)	13 (7.6)	0.148 ns
III	148	54 (36.5)	17 (11.5)	66 (44.6)	11 (7.4)	0.760 ns
IV	22	14 (63.6)	0 (0)	8 (36.4)	0 (0)	0.016*
Primary tumor location						
Proximal	82	26 (31.7)	17 (20.7)	31 (37.8)	8 (9.8)	0.079 ns
Lymph node metastasis						
Positive	160	61 (38.1)	17 (10.6)	71 (44.4)	11 (6.9)	0.439 ns
Lymphatic invasion						
Positive	245	91 (37.1)	28 (11.4)	112 (45.7)	14 (5.7)	0.088 ns
Venous invasion						
Positive	91	32 (35.2)	5 (5.5)	49 (53.8)	5 (5.5)	0.020*
Histology type						
Undifferentiated (por, muc)	22	4 (18.2)	1 (4.5)	14 (63.6)	3 (13.6)	0.069 ns

Proximal: Cecum and ascending colon.
por: Poorly differentiated adenocarcinoma.
muc: Mucinous adenocarcinoma.

Values are mean (standard deviation) or number (%).

I

Variables	Odds ratio	95% CI	p value
aPKCs expression	0.44	0.24-0.78	0.006**
Undifferentiated	0.75	0.25-2.78	0.622 ns
Lymphatic invasion	1.59	0.86-2.92	0.135 ns
Venous invasion	2.35	1.07-5.71	0.042 ns
Proximal origin	0.46	0.26-0.85	0.012*

0.1 1 10

Associated with HA negative | Associated with HA positive

J

Variables	Odds ratio	95% CI	p value
HA expression	0.45	0.24-0.80	0.007**
Undifferentiated	0.29	0.09-0.79	0.022*
Lymphatic invasion	1.12	0.66-1.90	0.685 ns
Venous invasion	0.67	0.39-1.15	0.150 ns
Proximal origin	1.04	0.61-1.78	0.880 ns

0.01 0.1 1 10

Associated with aPKCs low | Associated with aPKCs high

K

Variables	HR	95%CI	p value
aPKCs-HA expression status			
aPKCs-high/HA-positive	1 (reference)		
aPKCs-low/HA-positive	2.40	1.27-4.87	0.010**
aPKCs-high/HA-negative	0.51	0.07-1.90	0.379 ns
aPKCs-low/HA-negative	0.43	0.02-2.20	0.417 ns
Age ≥65 years old	2.70	1.41-5.51	0.004**
Histology type (undifferentiated)	2.73	1.14-5.84	0.015*
Lymph node metastasis (positive)	3.53	1.84-7.33	0.000***
Metastasis (positive)	2.68	1.07-5.80	0.020*
Primary tumor location (proximal)	1.13	0.57-2.15	0.710 ns

Figure S1. aPKCs expression correlates with mesenchymal features and HA deposition in human CRC, related to Figure 1

(A-D) Pie chart of CMS relative distribution (A), iCMS2 and iCMS3 score (B), MCP-counter scores for monocytic lineage, endothelium, and fibroblast (C), and volcano plot showing *HAS1* and *HAS2* as differentially expressed genes (D) of CRC TCGA samples according to aPKCs expression. Box and whiskers graphs indicate the median and the 25th and 75th percentiles, with minimum and maximum values at the extremes of the whiskers. Mann-Whitney test, *p < 0.05, **p < 0.01, ***p < 0.001, ****p < 0.0001.

(E) *HAS1* and *HAS2* mRNA levels according to aPKCs expression in CRC patients of the indicated datasets. Box and whiskers graphs indicate the median and the 25th and 75th percentiles, with minimum and maximum values at the extremes of the whiskers. Mann-Whitney test, and unpaired t-test. *p < 0.05, **p < 0.01, ***p < 0.001, ****p < 0.0001.

(F) Pearson correlation between HAS score and aPKC expression in CRC patients from TCGA.

(G) GSEA plots of enrichment in the indicated gene signatures in CRC patient samples from TCGA according to HAS score (n=301).

(H) Baseline clinical and pathological characteristics in four groups classified by tumoral aPKC expression and stromal HA deposition. One-way *ANOVA* test, *p < 0.05. ns: not significant.

(I and J) Multivariable logistic regression analyses for the factors associated with HA deposition (I) and aPKC expression (J). *p < 0.05, **p < 0.01. ns: not significant.

(K) Multivariable Cox proportional hazards regression analysis for overall survival. aPKC-high/HA-positive group was used as a reference to estimate the relative risks of the other three groups. 95%CI: 95% confidence intervals, HR: hazard ratios. Box and whiskers graphs indicate the median and the 25th and 75th percentiles, with minimum and maximum values at the extremes of the whiskers. *p < 0.05, **p < 0.01, ***p < 0.001, ****p < 0.0001. ns: not significant.

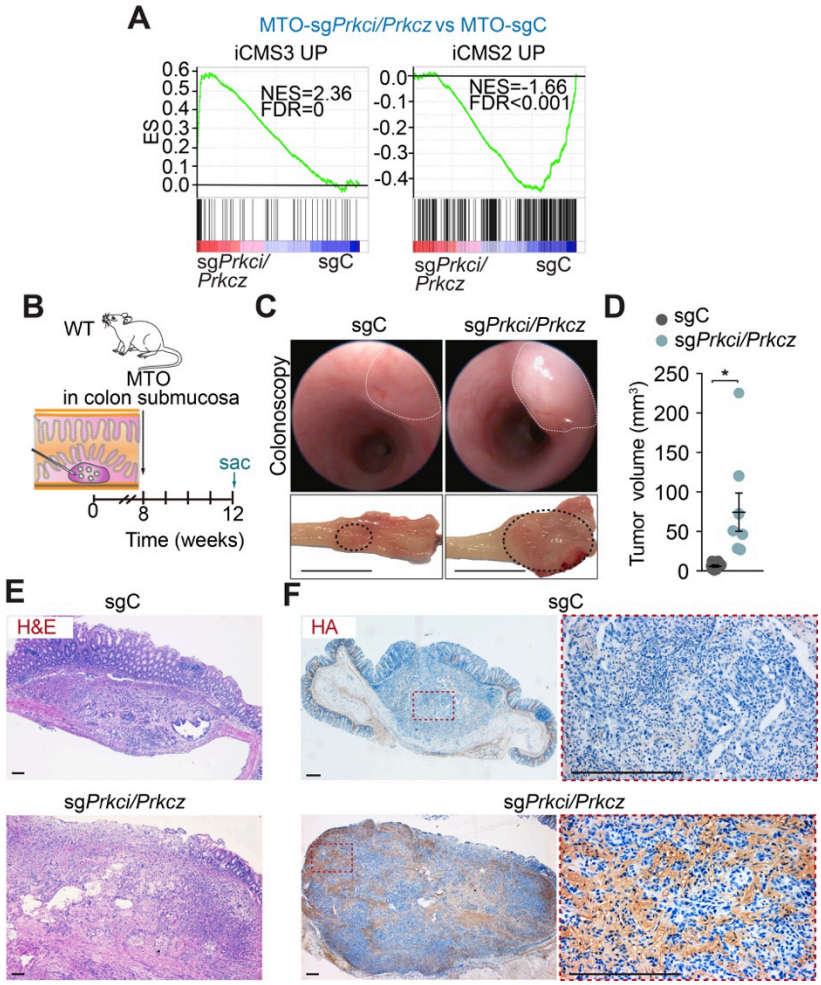

Figure S2. aPKC promotes HA deposition *in vivo* in orthotopic MTO transplantation, related to Figure 2

(A) GSEA plots of enrichment in the indicated gene signatures in MTO-sg*Prkci*/*Prkcz* vs MTO-sgC (n=3).

(B-F) Colonoscopy-guided orthotopic transplantation of MTO-sg*Prkci*/*Prkcz* (n=6) and MTO-sgC (n=6) in WT mice. Experimental design (B), colonoscopy (top), and colonic macroscopic images (bottom) of tumors generated in the colon submucosa by injection of MTO-sg*Prkci*/*Prkcz* and MTO-sgC (C), tumor volume (D), Hematoxylin and eosin (H&E) (E) and IHC for HA (F) of colon sections from MTO-sg*Prkci*/*Prkcz* and MTO-sgC. Unpaired t-test. Data shown as mean ± SEM, (n=8), *p < 0.05. Scale bars, 50 μm. Sac: sacrificed

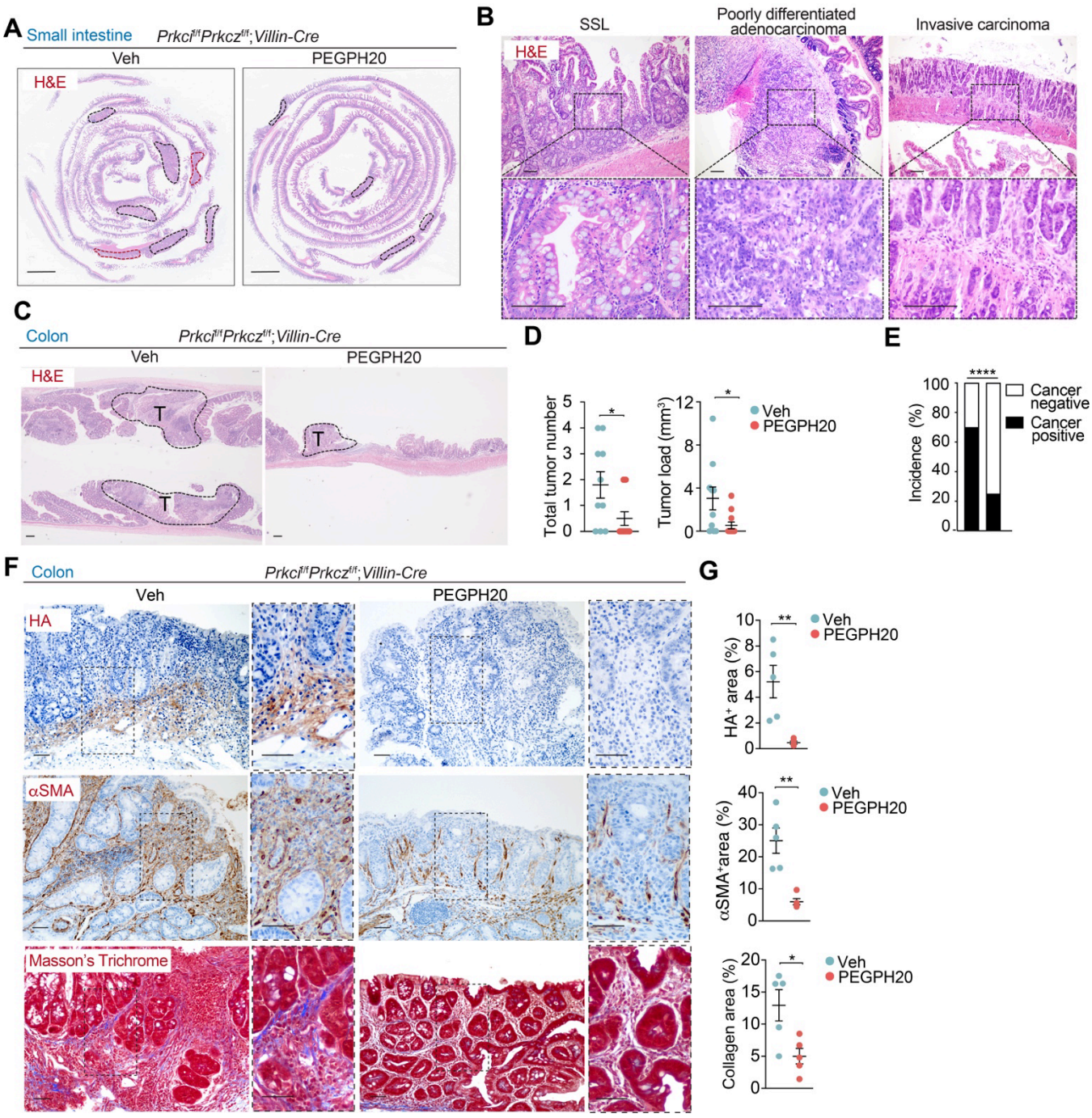

Figure S3. Degradation of hyaluronan by PEGPH20 treatment reduces *Prkci*$^{f/f}$*Prkcz*$^{f/f}$;*Villin-Cre* intestinal and colon tumors, related to Figure 3

(A) H&E staining, red lines mark tumor and black lines SSL of small intestine sections from *Prkci*$^{f/f}$*Prkcz*$^{f/f}$;*Villin-Cre* mice treated with Veh (n=10) or PEGPH20 (n=12). Scale bars, 2 mm.

(B) Representative H&E images of SSL, poorly differentiated adenocarcinoma, and invasive carcinoma of small intestine sections from *Prkci*$^{f/f}$*Prkcz*$^{f/f}$;*Villin-Cre* mice treated with Veh (n=10) or PEGPH20 (n=12). Scale bars, 100 μm.

(C-E) H&E staining (C), total tumor number, tumor load, unpaired t-test, data shown as mean ± SEM, *p < 0.05 (D), and quantification of cancer incidence, chi-square test, ****p < 0.0001 (E) from colon of *Prkci*$^{f/f}$*Prkcz*$^{f/f}$;*Villin-Cre* mice treated with Veh (n=10) or PEGPH20 (n=12). Black lines mark tumor. T: tumor. Scale bars, 200 μm.

(F-G) IHC for HA, αSMA, and Masson's trichrome (F) and staining quantification (G) from colon of *Prkci*$^{f/f}$*Prkcz*$^{f/f}$;*Villin-Cre* mice treated with Veh (n=5) or PEGPH20 (n=3). Mann-Whitney test, data shown as mean ± SEM, *p < 0.05, **p < 0.01. Scale bars, 50 μm.

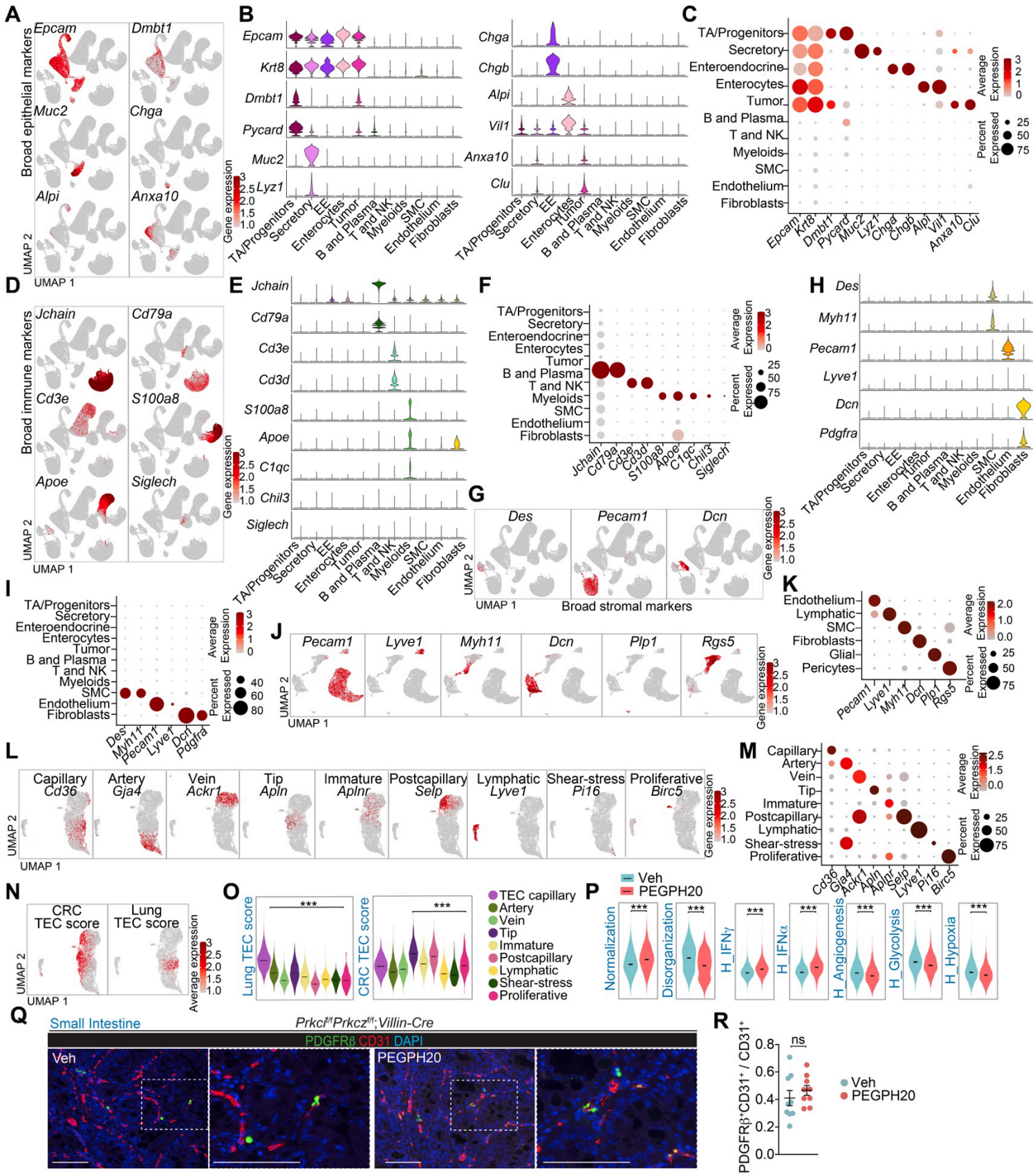
A
Broad epithelial markers
Epcam
Dmbt1
Muc2
Chga
Alpi
Anxa10
UMAP 1
UMAP 2
B
Epcam
Krt8
Dmbt1
Pycard
Muc2
Lyz1
Chga
Chgb
Alpi
Vil1
Anxa10
Clu
Gene expression
TA/Progenitors
Secretory
EE
Enterocytes
Tumor
B and Plasma
T and NK
Myeloids
SMC
Endothelium
Fibroblasts
C
Average Expression
Percent Expressed
D
Broad immune markers
Jchain
Cd79a
Cd3e
S100a8
Apoe
Siglech
E
Cd3d
C1qc
Chil3
F
Jchain
Cd79a
Cd3e
Cd3d
S100a8
Apoe
C1qc
Chil3
Siglech
G
Des
Pecam1
Dcn
Broad stromal markers
H
Des
Myh11
Pecam1
Lyve1
Dcn
Pdgfra
I
Des
Myh11
Pecam1
Lyve1
Dcn
Pdgfra
J
Pecam1
Lyve1
Myh11
Dcn
Plp1
Rgs5
K
Endothelium
Lymphatic
SMC
Fibroblasts
Glial
Pericytes
L
Capillary
Cd36
Artery
Gja4
Vein
Ackr1
Tip
Apln
Immature
Aplnr
Postcapillary
Selp
Lymphatic
Lyve1
Shear-stress
Pi16
Proliferative
Birc5
M
Capillary
Artery
Vein
Tip
Immature
Postcapillary
Lymphatic
Shear-stress
Proliferative
Cd36
Gja4
Ackr1
Apln
Aplnr
Selp
Lyve1
Pi16
Birc5
N
CRC TEC score
Lung TEC score
Average expression
O
Lung TEC score
CRC TEC score
***
TEC capillary
Artery
Vein
Tip
Immature
Postcapillary
Lymphatic
Shear-stress
Proliferative
P
Veh
PEGPH20
Normalization
Disorganization
H_IFNγ
H_IFNα
H_Angiogenesis
H_Glycolysis
H_Hypoxia
Q
Small Intestine
Prkci^f/f Prkcz^f/f ;Villin-Cre
PDGFRβ CD31 DAPI
Veh
PEGPH20
R
PDGFRβ+CD31+ / CD31+
ns
Veh
PEGPH20

Figure S4. scRNA-seq of *Prkci*$^{f/f}$*Prkcz*$^{f/f}$;*Villin-Cre* tumors treated with PEGPH20, related to Figure 4

(A-C) UMAP feature plots colored by the expression of epithelial markers (A), violin plots (B) and dot plot (C) of indicated gene expression by cell type in all *Prkci*$^{f/f}$*Prkcz*$^{f/f}$;*Villin-Cre* cells. The top and bottom of the violin plots represent the minimal and maximal values, and the width is based on the kernel density estimate of the data, scaled to have the same width for all clusters.

(D-F) UMAP feature plots colored by the expression of immune markers (D), violin plot (E) and dot plot (F) of indicated gene expression by cell type in all *Prkci*$^{f/f}$*Prkcz*$^{f/f}$;*Villin-Cre* cells. The top and bottom of the violin plots represent the minimal and maximal values, and the width is based on the kernel density estimate of the data, scaled to have the same width for all clusters.

(G-I) UMAP feature plots colored by the expression of stromal markers (G), violin plot (H), and dot plot (I) of indicated gene expression by cell type in all *Prkci*$^{f/f}$*Prkcz*$^{f/f}$;*Villin-Cre* cells. The top and bottom of the violin plots represent the minimal and maximal values, and the width is based on the kernel density estimate of the data, scaled to have the same width for all clusters.

(J and K) UMAP feature plots colored by the expression of indicated stromal genes (J) and dot plot (K) of indicated genes by stromal cell type in *Prkci*$^{f/f}$*Prkcz*$^{f/f}$;*Villin-Cre* stromal cells.

(L-O) UMAP feature plots colored by the expression of indicated genes (L), dot plot of indicated gene expression by endothelial cell type (M), UMAP feature plots colored by the expression of indicated signatures (N), and violin plots for the indicated gene signatures in *Prkci*$^{f/f}$*Prkcz*$^{f/f}$;*Villin-Cre* endothelial cells. The top and bottom of the violin plots represent the minimal and maximal values, and the width is based on the kernel density estimate of the data, scaled to have the same width for all clusters. Horizontal lines represent median values. Unpaired t-test, ***$p < 0.001$.

(P) Violin plots for endothelial normalization and disorganization, IFNγ, IFNα, angiogenesis, glycolysis, and hypoxia signatures from H compilation (MSigDB) in endothelial cells re-clustered and split by treatment, Veh or PEGPH20. The top and bottom of the violin plots represent the minimal and maximal values, and the width is based on the kernel density estimate of the data, scaled to have the same width for all clusters. Horizontal lines represent median values. Unpaired t-test, ***$p < 0.001$.

(Q and R) IF of PDGFRβ (green) with CD31 (red) (Q) and quantification (R) in small intestine tumors of *Prkci*$^{f/f}$*Prkcz*$^{f/f}$;*Villin-Cre* mice treated with Veh (n=5) or PEGPH20 (n=5). Unpaired t-test, data shown as mean ± SEM. ns: not significant. Scale bar, 100 μm.

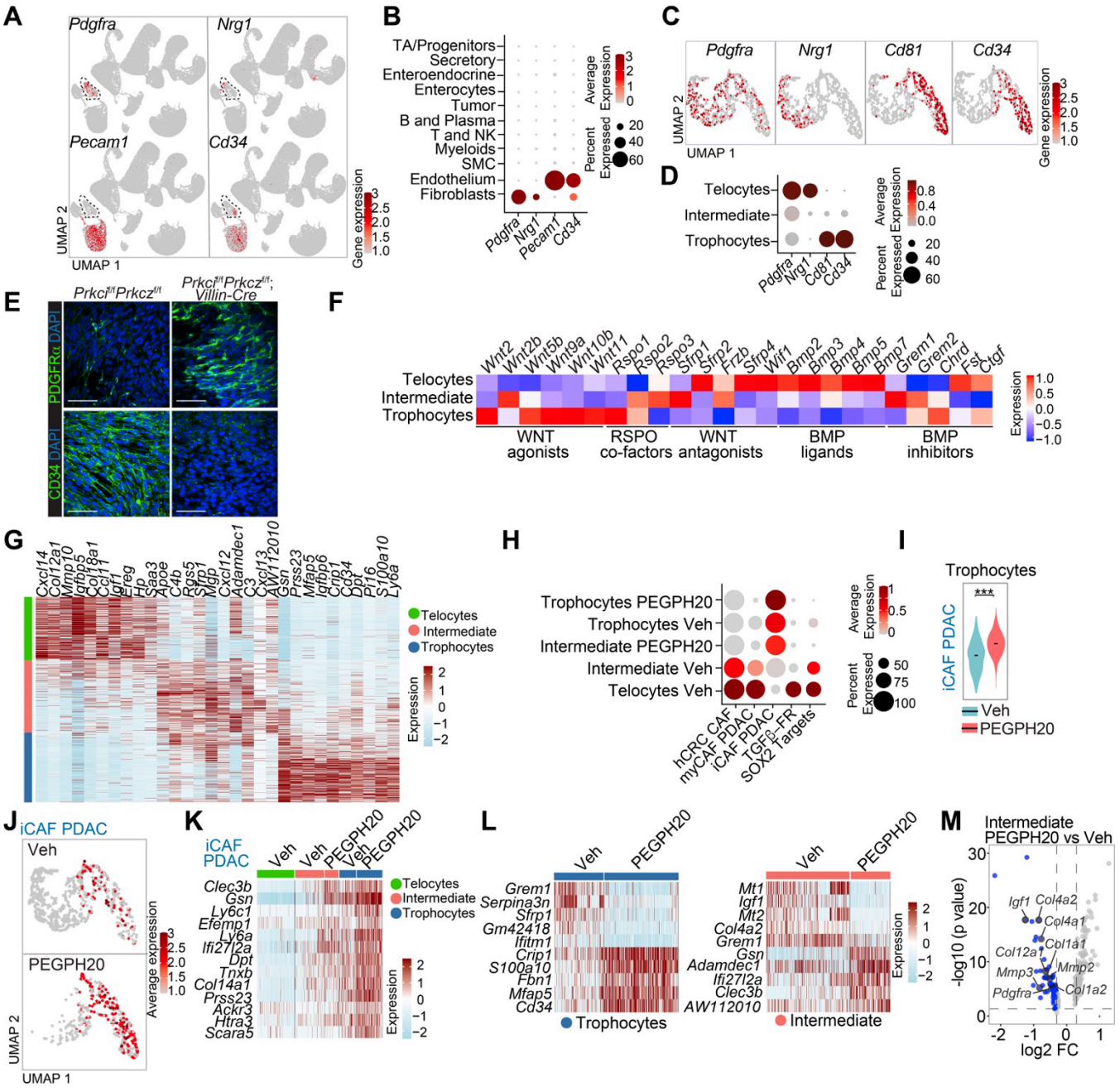

Figure S5. Fibroblast cell annotation and subpopulation characterization, related to Figure 4

(A and B) UMAP feature plots (A) and dot plot (B) of indicated stromal genes by cell type in all *Prkci*$^{f/f}$*Prkcz*$^{f/f}$;*Villin-Cre* cells. The dotted line outlines the fibroblast population in (A).

(C and D) UMAP feature plots (C), and dot plot of indicated gene expression by fibroblast cell type (D).

(E) IF of PDGFRα and CD34 in *Prkci*$^{f/f}$*Prkcz*$^{f/f}$ and *Prkci*$^{f/f}$*Prkcz*$^{f/f}$;*Villin-Cre* fibroblasts. Scale bars, 100 μm.

(F) Heatmap of average expression levels of the indicated genes in *Prkci*$^{f/f}$*Prkcz*$^{f/f}$;*Villin-Cre* fibroblasts.

(G) Heatmap of biomarkers of *Prkci*$^{f/f}$*Prkcz*$^{f/f}$;*Villin-Cre* fibroblasts populations.

(H) Dot plot of indicated gene signatures in Veh- or PEGPH20-treated *Prkci*$^{f/f}$*Prkcz*$^{f/f}$;*Villin-Cre* fibroblasts.

(I and J) Violin plot (I) in trophocytes and UMAP feature plots (J) in fibroblasts split by treatment, Veh or PEGPH20, colored by the expression of iCAF PDAC signature. The top and bottom of the violin plots represent the minimal and maximal values, and the width is based on the kernel density estimate of the data, scaled to have the same width for all clusters. Horizontal lines represent median values. Unpaired t-test, ***$p < 0.001$.

(K) Heatmap of gene expression from iCAF PDAC signature in *Prkci*$^{f/f}$*Prkcz*$^{f/f}$;*Villin-Cre* fibroblasts populations split by treatment, Veh or PEGPH20.

(L) Heatmap of top 10 differentially expressed genes in trophocytes or intermediate fibroblasts treated with PEGPH20 versus Veh.

(M) Volcano plot of differentially expressed genes in intermediate fibroblasts treated with PEGPH20 versus Veh intermediate fibroblast.

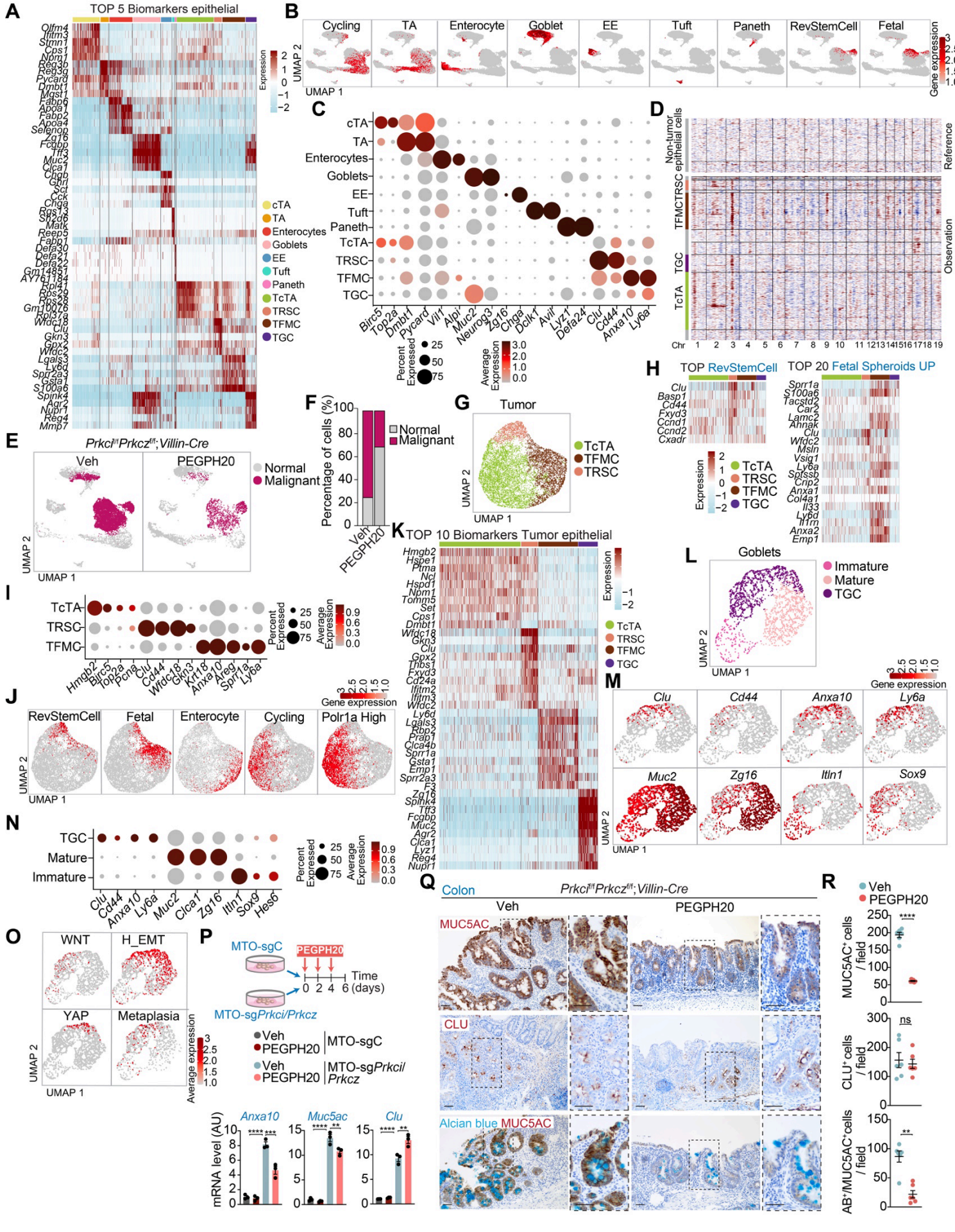
A
TOP 5 Biomarkers epithelial
Olfm4
Ifitm3
Stmn1
Ccs1
Npm1
Reg3b
Reg3g
Pycard
Dmbt1
Mgst1
Fabp6
Apoa1
Fabp2
Apoa4
Selenop
Zg16
Fcgbp
Tff3
Muc2
Clca1
Chgb
Ghrl
Sct
Cck
Chga
Ras13
Sh2d6
Matk
Reep5
Fabp1
Defa30
Defa21
Defa22
Gm14851
AY761184
Rpl41
Rps29
Rps28
Gm10076
Rpl37a
Wfdc18
Clu
Gkn3
Gpx2
Wfdc2
Lgals3
Ly6d
Sprr2a3
Gsta1
S100a6
Spink4
Agr2
Nupr1
Reg4
Mmp7
Expression
2
1
0
−1
−2
B
Cycling
TA
Enterocyte
Goblet
EE
Tuft
Paneth
RevStemCell
Fetal
UMAP 2
UMAP 1
Gene expression
3
2.5
2.0
1.5
1.0
C
cTA
TA
Enterocytes
Goblets
EE
Tuft
Paneth
TcTA
TRSC
TFMC
TGC
Birc5
Top2a
Dmbt1
Pycard
Vil1
Alpi
Muc2
Neurog3
Zg16
Chga
Dclk1
Avil
Lyz1
Defa24
Clu
Cd44
Anxa10
Ly6a
Percent Expressed
25
50
75
Average Expression
3.0
2.0
1.0
0.0
D
Non-tumor epithelial cells
TFMC
TRSC
TGC
TcTA
Reference
Observation
Chr 1 2 3 4 5 6 7 8 9 10 11 12 13 14 15 16 17 18 19
E
Prkci f/f Prkcz f/f ;Villin-Cre
Veh
PEGPH20
Normal
Malignant
UMAP 2
UMAP 1
F
Percentage of cells (%)
100
80
60
40
20
0
Normal
Malignant
Veh
PEGPH20
G
Tumor
TcTA
TFMC
TRSC
UMAP 2
UMAP 1
H
TOP RevStemCell
TOP 20 Fetal Spheroids UP
Clu
Basp1
Cd44
Fxyd3
Ccnd1
Ccnd2
Cxadr
Sprr1a
S100a6
Tacstd2
Car2
Lamc2
Ahnak
Clu
Wfdc2
Msln
Vsig1
Ly6a
Sptssb
Crip2
Anxa1
Col4a1
Il33
Ly6d
Il1rn
Anxa2
Emp1
Expression
2
1
0
−1
−2
TcTA
TRSC
TFMC
TGC
I
TcTA
TRSC
TFMC
Hmgb2
Birc5
Top2a
Pcna
Clu
Cd44
Wfdc18
Gkn3
Krt18
Anxa10
Areg
Sprr1a
Ly6a
Percent Expressed
25
50
75
Average Expression
0.9
0.6
0.3
0.0
J
Gene expression
3
2.5
2.0
1.5
1.0
RevStemCell
Fetal
Enterocyte
Cycling
Polr1a High
UMAP 2
UMAP 1
K
TOP 10 Biomarkers Tumor epithelial
Hmgb2
Hspe1
Ptma
Ncl
Hspd1
Npm1
Tomm5
Set
Cps1
Dmbt1
Wfdc18
Gkn3
Clu
Gpx2
Thbs1
Fxyd3
Cd24a
Ifitm2
Ifitm3
Wfdc2
Ly6d
Lgals3
Rbp2
Prap1
Clca4b
Sprr1a
Gsta1
Emp1
Sprr2a3
F3
Zg16
Spink4
Tff3
Fcgbp
Muc2
Agr2
Clca1
Lyz1
Reg4
Nupr1
Expression
−1
−2
TcTA
TRSC
TFMC
TGC
L
Goblets
Immature
Mature
TGC
UMAP 2
UMAP 1
M
Gene expression
3
2.5
2.0
1.5
1.0
Clu
Cd44
Anxa10
Ly6a
Muc2
Zg16
Itln1
Sox9
UMAP 2
UMAP 1
N
TGC
Mature
Immature
Clu
Cd44
Anxa10
Ly6a
Muc2
Clca1
Zg16
Itln1
Sox9
Hes6
Percent Expressed
25
50
75
Average Expression
0.9
0.6
0.3
0.0
O
WNT
H_EMT
YAP
Metaplasia
UMAP 2
UMAP 1
Average expression
3
2.5
2.0
1.5
1.0
P
MTO-sgC
PEGPH20
Time
0 2 4 6 (days)
MTO-sgPrkci/Prkcz
Veh
PEGPH20
MTO-sgC
Veh
PEGPH20
MTO-sgPrkci/Prkcz
Anxa10
Muc5ac
Clu
mRNA level (AU)
****
***
**
Q
Colon
Prkci f/f Prkcz f/f ;Villin-Cre
Veh
PEGPH20
MUC5AC
CLU
Alcian blue MUC5AC
R
Veh
PEGPH20
MUC5AC+ cells / field
****
CLU+ cells / field
ns
AB+/MUC5AC+cells / field
**

Figure S6. Tumor epithelial cell annotation and subpopulation characterization, related to Figure 5

(A-C) Heatmap of top 5 biomarkers (A), UMAP feature plots colored by the expression of indicated gene signatures (B), and dot plot (C) of indicated epithelial markers by epithelial cell type in *Prkci*$^{f/f}$*Prkcz*$^{f/f}$;*Villin-Cre* epithelial cells.

(D) Inferred large-scale copy number variations (CNVs) identifying TcTA, TRSC, TFMC, TGC and non-cancer cells. Epithelial and spike in control cells are included on the y-axis and chromosomal regions on the x-axis. Amplifications (red) or deletions (blue) were inferred by averaging expression over 100-gene stretches on the respective chromosome.

(E and F) UMAP of epithelial cells colored by inferred cell malignancy identity (E) and malignant epithelial cell percentage relative to the total epithelial cells count per treatment (F) in *Prkci*$^{f/f}$*Prkcz*$^{f/f}$; *Villin-Cre* tumors.

(G) UMAP tumor epithelial cells colored by tumor epithelial cell type in all *Prkci*$^{f/f}$*Prkcz*$^{f/f}$;*Villin-Cre* tumors.

(H) Heatmap of gene expression of the indicated gene signatures of *Prkci*$^{f/f}$*Prkcz*$^{f/f}$;*Villin-Cre* tumor epithelial cells.

(I) Dot plot of indicated gene expression by tumor epithelial cell type.

(J) UMAP feature plots colored by the expression of indicated signatures in *Prkci*$^{f/f}$*Prkcz*$^{f/f}$;*Villin-Cre* tumor epithelial cells.

(K) Heatmap of top 10 biomarkers of *Prkci*$^{f/f}$*Prkcz*$^{f/f}$;*Villin-Cre* tumor epithelial cells.

(L and M) UMAP goblet cells colored by goblet cell type (L) and colored by the expression of indicated genes (M) in *Prkci*$^{f/f}$*Prkcz*$^{f/f}$;*Villin-Cre* goblet cells.

(N) Dot plot of indicated gene expression by goblet cell type.

(O) UMAP feature plots colored by the expression of indicated signatures in *Prkci*$^{f/f}$*Prkcz*$^{f/f}$;*Villin-Cre* goblet cells.

(P) Schematic representation of PEGPH20 treatment in mouse tumor organoids (MTO) and qPCR of indicated genes in Veh- and PEGPH20-treated MTO. One-way *ANOVA* and *post hoc Tukey's* test. Data shown as mean ± SEM (n=3 biological replicates). **p < 0.01, ***p < 0.001, ****p < 0.0001.

(Q and R) IHC for MUC5AC, CLU, and Alcian blue with MUC5AC (Q) and staining quantification (R) from colon of *Prkci*$^{f/f}$*Prkcz*$^{f/f}$;*Villin-Cre* mice treated with Veh (n=5) or PEGPH20 (n=3). Unpaired-t-test and Mann-Whitney, data shown as mean ± SEM. **p < 0.01, ****p < 0.0001. Scale bar, 50 μm.

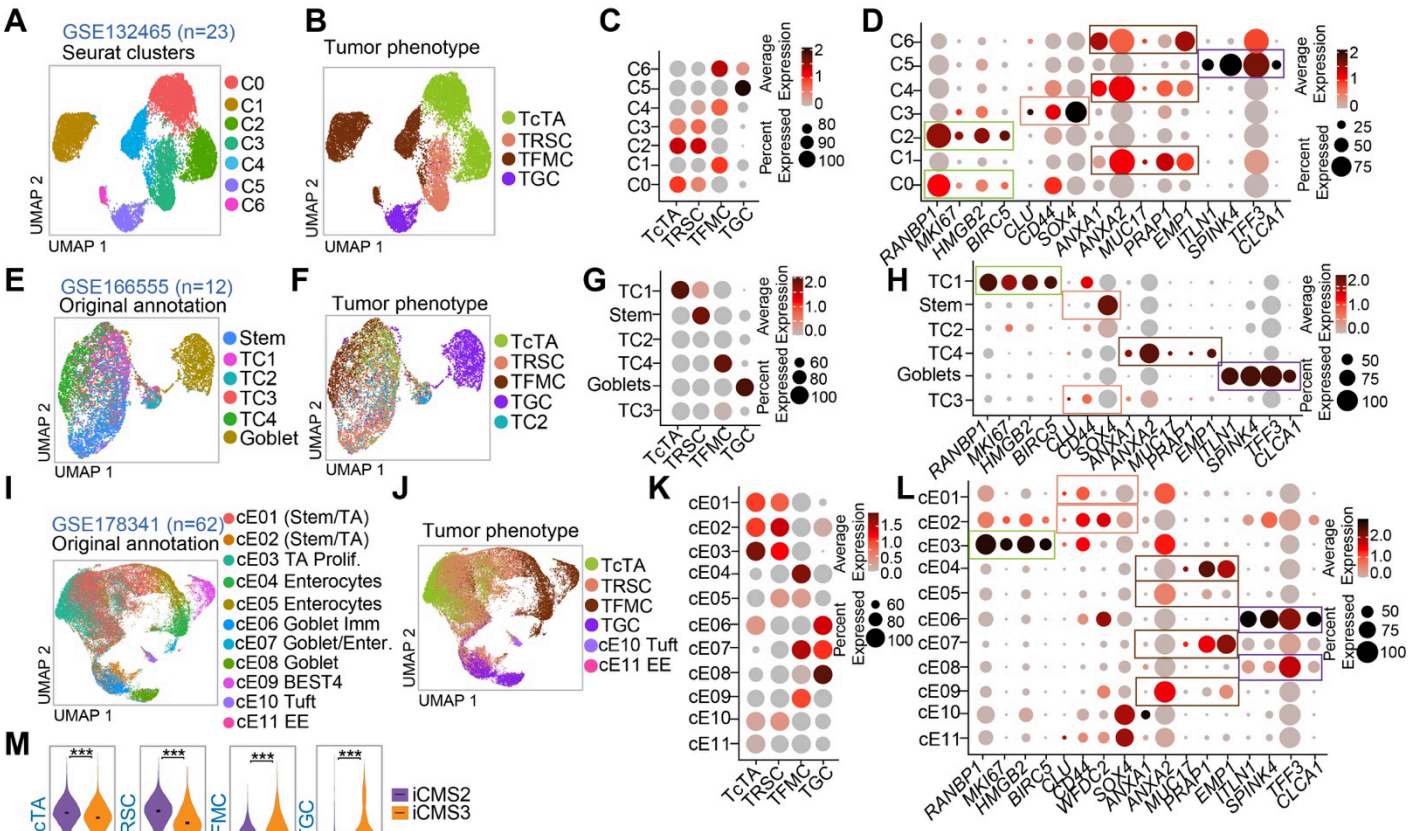

O

Variables	HR	95%CI	p value
ANXA10 high	3.13	1.68-5.80	0.000***
Age ≥65 years old	2.69	1.40-5.51	0.004 **
Histology type (undifferentiated)	2.35	0.97-5.10	0.041*
Lymph node metastasis (positive)	4.35	2.23-9.15	<0.000****
Metastasis (positive)	3.99	1.57-8.91	0.002**
Primary tumor location (proximal)	0.93	0.46-1.78	0.852 ns

Q

Variables	Odds ratio	Odds ratio	95% CI	P value
ANXA10 expression		1.87	1.11-3.16	0.018*
Undifferentiated		1.98	0.79-5.29	0.153 ns
Lymphatic invasion		1.15	0.67-1.98	0.611 ns
Venous invasion		1.69	0.99-2.90	0.054 ns
Proximal origin		0.70	0.40-1.19	0.189 ns

0.1 1 10
Associated with the rest | Associated with aPKCs-low HA-positive

P

Variables	HR	95%CI	p value
MUC5AC positive	2.86	1.51-5.40	0.001**
Age ≥65 years old	2.75	1.45-5.61	0.003 **
Histology type (undifferentiated)	1.97	0.79-4.40	0.117
Lymph node metastasis (positive)	4.04	2.08-8.47	<0.000****
Metastasis (positive)	3.80	1.49-8.54	0.002**
Primary tumor location (proximal)	0.851	0.42-1.61	0.633 ns

R

Variables	Odds ratio	Odds ratio	95% CI	P value
MUC5AC expression		1.98	1.18-3.36	0.010*
Undifferentiated		1.66	0.65-4.49	0.298 ns
Lymphatic invasion		1.17	0.68-2.02	0.567 ns
Venous invasion		1.87	1.09-3.23	0.023*
Proximal origin		0.67	0.39-1.14	0.146 ns

0.1 1 10
Associated with the rest | Associated with aPKCs-low HA-positive

Figure S7. scRNA-seq and TMA of human CRC tumors, related to Figure 5

(A-D) UMAP plots colored by seurat clusters (A) and by *Prkci*$^{f/f}$*Prkcz*$^{f/f}$;*Villin-Cre* tumor cell phenotypes (B); dot plots of *Prkci*$^{f/f}$*Prkcz*$^{f/f}$;*Villin-Cre* tumor epithelial gene signatures (C) and indicated genes (D) split by seurat clusters in tumor epithelial cells (GSE132465). Colored-coded boxes identify selected genes expressed in human cell populations that are present in *Prkci*$^{f/f}$*Prkcz*$^{f/f}$;*Villin-Cre* tumor cell phenotypes.

(E-H) UMAP plots colored by original annotation (E) and by *Prkci*$^{f/f}$*Prkcz*$^{f/f}$;*Villin-Cre* tumor cell phenotypes (F), dot plots of *Prkci*$^{f/f}$*Prkcz*$^{f/f}$;*Villin-Cre* tumor epithelial gene signatures split by original annotation cell types (G), and of indicated genes split by original annotation clusters (H) in tumor epithelial cells (GSE166555). Colored-coded boxes identify selected genes expressed in human cell populations that are present in *Prkci*$^{f/f}$*Prkcz*$^{f/f}$;*Villin-Cre* tumor cell phenotypes.

(I-L) UMAP plots colored by original annotation (I) and by *Prkci*$^{f/f}$*Prkcz*$^{f/f}$;*Villin-Cre* tumor cell phenotypes (J), dot plots of *Prkci*$^{f/f}$*Prkcz*$^{f/f}$;*Villin-Cre* tumor epithelial gene signatures split by original annotation cell types (K), and of indicated genes split by original annotation clusters (L) in tumor epithelial cells (GSE178341). Colored-coded boxes identify selected genes expressed in human cell populations that are present in *Prkci*$^{f/f}$*Prkcz*$^{f/f}$;*Villin-Cre* tumor cell phenotypes.

(M) Violin plots of *Prkci*$^{f/f}$*Prkcz*$^{f/f}$;*Villin-Cre* tumor epithelial gene signatures split by iCMS subtype, by sidedness, or by TNM stage of CRC tumors (GSE132465). The top and bottom of the violin plots represent the minimal and maximal values, and the width is based on the kernel density estimate of the data, scaled to have the same width for all clusters. Horizontal lines represent median values. Unpaired t-test, ***$p < 0.001$.

(N) Kaplan-Meier curve for overall survival of CRC patients according to ANXA10 or MUC5AC expression, Log-rank test (n=338).

(O-R) Multivariable Cox proportional hazards regression analysis for 8-year overall survival with ANXA10 high (O) or MUC5AC positive (P) expression. Multivariable logistic regression analysis for the factors associated with aPKC-low expression and positive HA deposition. Pathological factors and positive ANXA10 expression (Q) or positive MUC5AC expression (R) were analyzed for association. HR: hazard ratios, 95%CI: 95% confidence intervals. *$p < 0.05$, **$p < 0.01$, ***$p < 0.001$, ****$p < 0.0001$. ns: not significant.

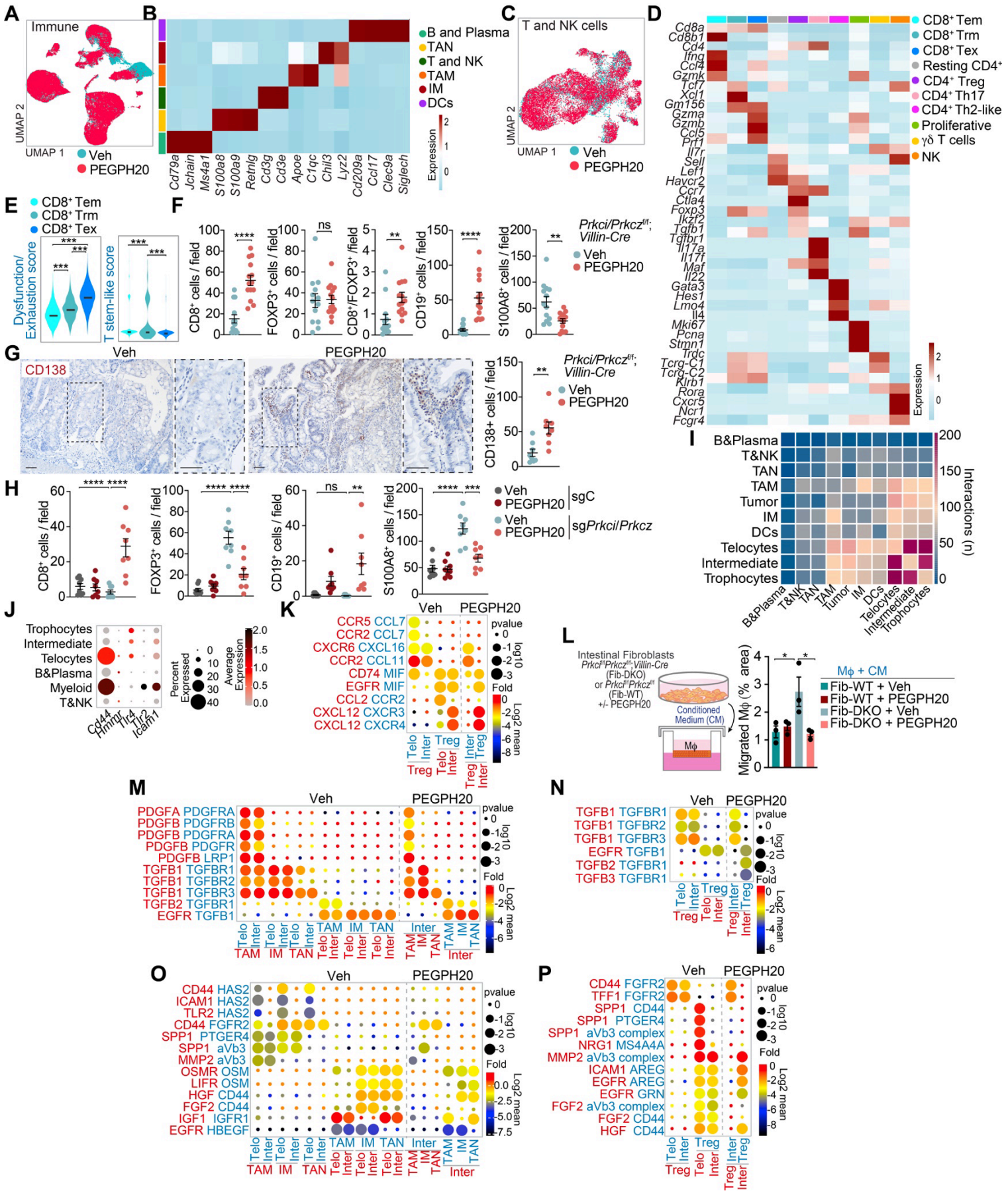
A
Immune
UMAP 2
UMAP 1
Veh
PEGPH20
B
B and Plasma
TAN
T and NK
TAM
IM
DCs
Expression
Cd79a
Jchain
Ms4a1
S100a8
S100a9
Retnlg
Cd3g
Cd3e
Apoe
C1qc
Chil3
Lyz2
Cd209a
Ccl17
Clec9a
Siglech
C
T and NK cells
UMAP 2
UMAP 1
Veh
PEGPH20
D
CD8+ Tem
CD8+ Trm
CD8+ Tex
Resting CD4+
CD4+ Treg
CD4+ Th17
CD4+ Th2-like
Proliferative
γδ T cells
NK
Cd8a
Cd8b1
Cd4
Ifng
Ccl4
Gzmk
Tcf7
Xcl1
Gm156
Gzma
Gzmb
Ccl5
Prf1
Il7r
Sell
Lef1
Havcr2
Ccr7
Ctla4
Foxp3
Ikzf2
Tgfb1
Tgfbr1
Il17a
Il17f
Maf
Il22
Gata3
Hes1
Lmo4
Il4
Mki67
Pcna
Stmn1
Trdc
Tcrg-C1
Tcrg-C2
Klrb1
Rora
Cxcr5
Ncr1
Fcgr4
Expression
E
CD8+ Tem
CD8+ Trm
CD8+ Tex
Dysfunction/ Exhaustion score
T stem-like score
F
Prkci/Prkcz f/f; Villin-Cre
Veh
PEGPH20
CD8+ cells / field
FOXP3+ cells / field
CD8+/FOXP3+ /field
CD19+ cells / field
S100A8+ cells / field
G
CD138
Veh
PEGPH20
CD138+ cells / field
Prkci/Prkcz f/f; Villin-Cre
H
CD8+ cells / field
FOXP3+ cells / field
CD19+ cells / field
S100A8+ cells / field
Veh
PEGPH20
sgC
Veh
PEGPH20
sgPrkci/Prkcz
I
B&Plasma
T&NK
TAN
TAM
Tumor
IM
DCs
Telocytes
Intermediate
Trophocytes
Interactions (n)
J
Trophocytes
Intermediate
Telocytes
B&Plasma
Myeloid
T&NK
Cd44
Hmmr
Tlr4
Tlr2
Icam1
Percent Expressed
Average Expression
K
Veh
PEGPH20
CCR5 CCL7
CCR2 CCL7
CXCR6 CXCL16
CCR2 CCL11
CD74 MIF
EGFR MIF
CCL2 CCR2
CXCL12 CXCR3
CXCL12 CXCR4
pvalue
log10
Fold
Log2 mean
Telo
Inter
Treg
L
Intestinal Fibroblasts
Prkci f/fPrkcz f/f;Villin-Cre
(Fib-DKO)
or Prkci f/fPrkcz f/f
(Fib-WT)
+/- PEGPH20
Conditioned Medium (CM)
Mϕ
Migrated Mϕ (% area)
Mϕ + CM
Fib-WT + Veh
Fib-WT + PEGPH20
Fib-DKO + Veh
Fib-DKO + PEGPH20
M
Veh
PEGPH20
PDGFA PDGFRA
PDGFB PDGFRB
PDGFB PDGFRA
PDGFB PDGFR
PDGFB LRP1
TGFB1 TGFBR1
TGFB1 TGFBR2
TGFB1 TGFBR3
TGFB2 TGFBR1
EGFR TGFB1
Telo
Inter
TAM
IM
TAN
N
Veh
PEGPH20
TGFB1 TGFBR1
TGFB1 TGFBR2
TGFB1 TGFBR3
EGFR TGFB1
TGFB2 TGFBR1
TGFB3 TGFBR1
O
Veh
PEGPH20
CD44 HAS2
ICAM1 HAS2
TLR2 HAS2
CD44 FGFR2
SPP1 PTGER4
SPP1 aVb3
MMP2 aVb3
OSMR OSM
LIFR OSM
HGF CD44
FGF2 CD44
IGF1 IGFR1
EGFR HBEGF
P
Veh
PEGPH20
CD44 FGFR2
TFF1 FGFR2
SPP1 CD44
SPP1 PTGER4
SPP1 aVb3 complex
NRG1 MS4A4A
MMP2 aVb3 complex
ICAM1 AREG
EGFR AREG
EGFR GRN
FGF2 aVb3 complex
FGF2 CD44
HGF CD44

Figure S8. PEGPH20 alleviates immunosuppression and allows CD8$^+$ T cell infiltration, related to Figure 6

(A) UMAP of immune cells colored by treatment in *Prkci*$^{f/f}$*Prkcz*$^{f/f}$;*Villin-Cre* tumors.

(B) Heatmap of average expression of B and plasma cells, tumor-associated neutrophils (TANs), T and NK cells, tumor-associated macrophages (TAMs), dendritic cells (DCs), and inflammatory monocytes (IMs) marker genes across immune cells subset in scRNA-seq data.

(C) UMAP of T cells colored by treatment in *Prkci*$^{f/f}$*Prkcz*$^{f/f}$;*Villin-Cre* tumors.

(D) Heatmap of average expression of CD8$^+$ Tem, CD8$^+$ Trm, CD8$^+$ Tex, resting CD4$^+$ T, CD4$^+$ Treg, CD4$^+$ Th17, CD4$^+$ Th2-like, proliferative, γδ and NK cells marker genes across T cell subset in scRNA-seq data.

(E) Violin plots for the indicated gene signatures in CD8$^+$ Tem, CD8$^+$ Trm, and CD8$^+$ Tex cells. The top and bottom of the violin plots represent the minimal and maximal values, and the width is based on the kernel density estimate of the data, scaled to have the same width for all clusters. Horizontal lines represent median values. Unpaired t-test, ***p < 0.001.

(F) Quantification of immune cell populations of *Prkci*$^{f/f}$*Prkcz*$^{f/f}$;*Villin-Cre* Veh- or PEGPH20-treated tumors (n=3) of Figure 6I, unpaired t-test and Mann-Whitney, data shown as mean ± SEM, **p < 0.01, ****p < 0.0001.

(G) CD138 staining and quantification from *Prkci*$^{f/f}$*Prkcz*$^{f/f}$;*Villin-Cre* Veh- or PEGPH20-treated tumors (n=3) of the experiment of Figure 2F, unpaired t-test, data shown as mean ± SEM, **p < 0.01.

(H) Quantification of the immune cell populations of Veh- or PEGPH20-treated tumors from MTO-sg*Prkci*/*Prkcz* and MTO-sgC, one-way *ANOVA* and *post hoc Tukey's* test, data shown as mean ± SEM, **p < 0.01, ***p < 0.001, ****p < 0.0001.

(I and J) CellphoneDB analysis of the number of ligand-receptor interactions between fibroblast and immune cells (I) and dot plot of HA receptors for fibroblast and immune cells (J) in *Prkci*$^{f/f}$*Prkcz*$^{f/f}$;*Villin-Cre* Veh-treated tumors.

(K) CellphoneDB analysis of ligand-receptor pairs of cytokines between telocytes, intermediate and CD4$^+$Treg cells in *Prkci*$^{f/f}$*Prkcz*$^{f/f}$;*Villin-Cre* Veh- and PEGPH20-treated tumors.

(L) Experimental design and migration of bone marrow macrophages stimulated by CM of intestinal fibroblasts with or without PEGPH20 (n=3), unpaired t-test, data shown as mean ± SEM, *p < 0.05.

(M and N) CellphoneDB analysis of ligand-receptor pairs of PDGFR/TGFβ signaling between telocytes, intermediate with myeloid cells (M) or CD4$^+$ Treg (N) in *Prkci*$^{f/f}$*Prkcz*$^{f/f}$;*Villin-Cre* Veh- and PEGPH20-treated tumors.

(O and P) CellphoneDB analysis of ligand-receptor pairs of network genes of HA signaling between telocytes, intermediate with myeloid cells (O) or CD4$^+$ Treg (P) in *Prkci*$^{f/f}$*Prkcz*$^{f/f}$;*Villin-Cre* Veh- and PEGPH20-treated tumors.

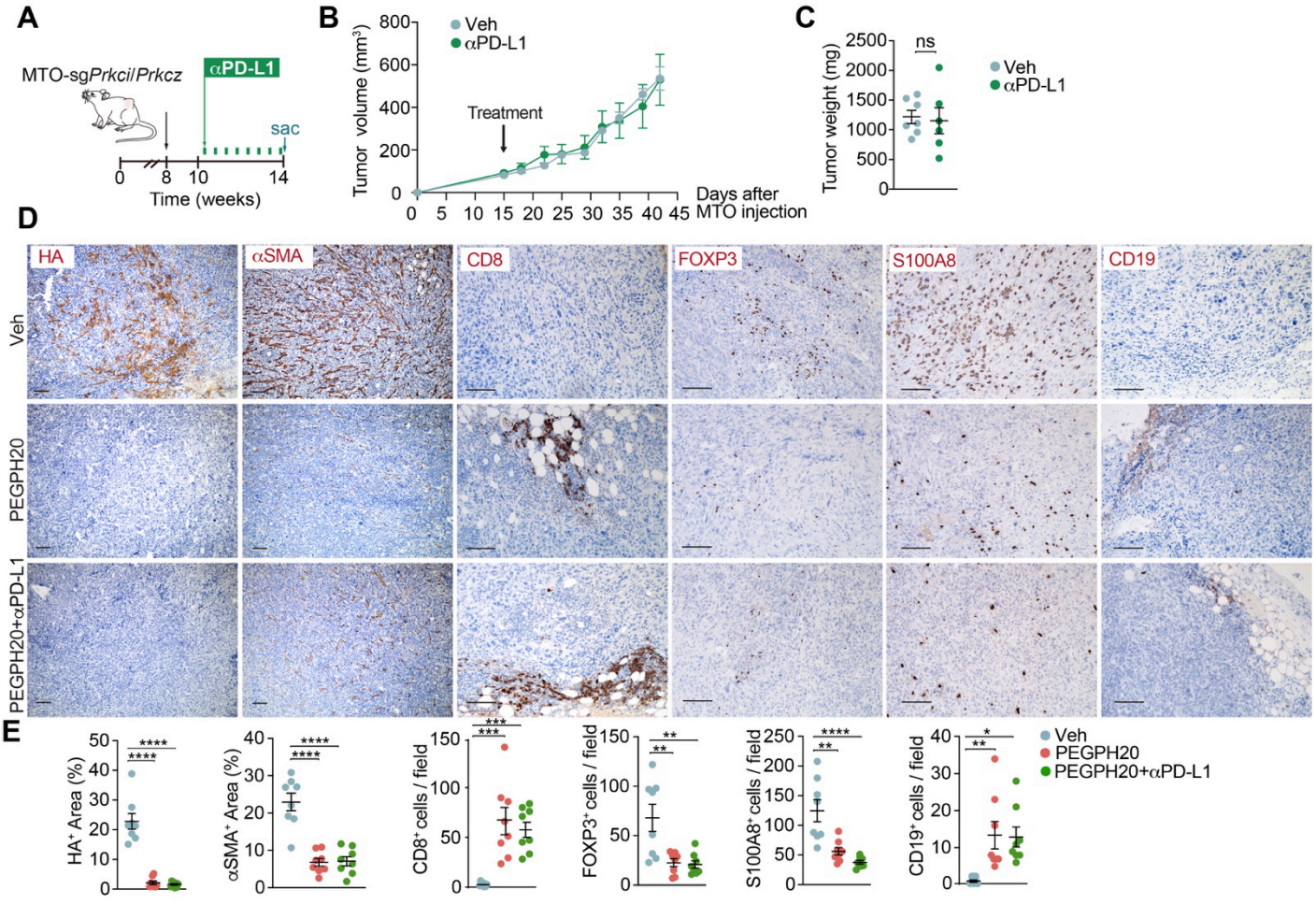
A
MTO-sgPrkci/Prkcz
αPD-L1
sac
0
8
10
14
Time (weeks)
B
Veh
αPD-L1
Tumor volume (mm3)
Treatment
Days after MTO injection
C
ns
Tumor weight (mg)
Veh
αPD-L1
D
HA
αSMA
CD8
FOXP3
S100A8
CD19
Veh
PEGPH20
PEGPH20+αPD-L1
E
HA+ Area (%)
αSMA+ Area (%)
CD8+ cells / field
FOXP3+ cells / field
S100A8+ cells / field
CD19+ cells / field
Veh
PEGPH20
PEGPH20+αPD-L1

Figure S9. aPKC-deficient tumors are resistant to ICB monotherapy, related to Figure 7

(A-C) Subcutaneous injection of MTO-sg*Prkci*/*Prkcz* in WT mice treated twice a week with αPD-L1 (5 mg/kg) for 4 weeks (n:Veh=7, PEGPH20-treated with αPD-L1-treated=6). Experimental design (A), tumor volume, two-way *ANOVA* and *post hoc Tukey's* test (B); tumor weight, unpaired t-test (C). Data shown as mean ± SEM. ns: not significant. Sac: sacrificed

(D and E) IHC for HA, αSMA, CD8, FOXP3, S100A8, and CD19 (D), and quantification (E) of tumors from mice treated as in Figure 7B. One-way *ANOVA* and *post hoc Tukey's* test, data shown as mean ± SEM, *p < 0.05, **p < 0.01, ***p < 0.001, ****p < 0.0001. Scale bars, 100 μm.

Table S1. List of primers used, Related to STAR Methods

Gene symbol	Forward	Reverse
18s	5'- GTAACCCGTTGAACCCCAT-3'	5'- CCATCCAATCGGTAGTAGCG-3'
Prkcz	5'-TGTGTCCTCACAGATGGAGC-3'	5'-TCCACGGCGGTAGATGGA-3'
Prkci	5'-GCGGGGATATTATGATAACACACTT-3'	5'-TTCCTCATCTATCCATTTCATGGT-3'
Has1	5'- GTGCGAGTGTTGGATGAAGACC-3'	5'-CCACATTGAAGGCTACCCAGTATC-3'
Has2	5'- GCCATTTTCCGAATCCAAACAGAC-3'	5'- CCTGCCACACTTATTGATGAGAACC-3'
Has3	5'-GCTTCAGTCCAGAAACCAAAGTAGG-3'	5'- CCTCGTTCCTCAAGAGAAACAAGG-3'
Anxa10	5'- TAGGCGGAGCACTCCAAGGATT-3'	5'- GCCATACATGCTCTGATAGGTCC-3'
Clu	5'- CTGTCCACTCAAGGGAGTAGG-3'	5'- GTGTCCTCCAGAGCATCCTC-3'
Muc5ac	5'- CCACTTTCTCCTTCTCCACACC-3'	5'- GGTTGTCGATGCAGCCTTGCTT-3'
HAS2	5'- AAACTGCTGCAAGAGGTTATTCCT-3'	5'- GTCATGTACACAGCCTTCAGAGC-3'

Table S2. List of guides, Related to STAR Methods

Guides	Source	Identifier
gRNA targeting human *PRKCI* 5'-TTAAATTATCTTCATGAGCG-3'	Synthego	N/A
gRNA targeting human *PRKCZ* 5'-CACCTGCAGAGAGCGTACTG-3'	Synthego	N/A
gRNA targeting mouse *Prkcz* 5'-CATCTACCGGGACCTAAAAC -3'	N/A	N/A